****
****

CHAPTER - VIII

VARIATION OF HARDNESS WITH LOAD

****
****

CHAPTER - VIII

VARIATION OF HARDNESS WITH LOAD

****
****
****
*****
***
*

8.1 INTRODUCTION :

It is clear from the discussion of the previous Chapter that ' Standard hardness ' 'a' is a function of quenching temperature ; 'a_1' and 'a_2' in general vary with quenching temperature (T_Q). However, the variation of a_1 with quenching temperature is more noticeable than that of a_2. In particular, a_1 in case of knoop indentation is more susceptible to quenching temperature than that of Vickers indentation. It is now interesting and useful to study in detail how hardness changes with quenching temperature.

The Knoop and Vickers hardness numbers (H_k and H_v) are defined by equations, (Mott, 1956)

$$\text{KHN,} \quad H_k = \frac{14230 \; P}{d^2} \qquad \ldots\ldots\ldots \quad (8.1)$$

$$\text{VHN,} \quad H_v = \frac{1854.4 \; P}{d^2} \qquad \ldots\ldots\ldots \quad (8.2)$$

where load P is measured in grams and the diagonal length d, of the indentation mark in microns. The hardness number is not an ordinary number, but a constant having dimensions and a deep, but less understood, physical meaning. The combination of these equations with

$$P = ad^n \qquad \ldots\ldots\ldots \quad (8.3)$$

yields,

$$H = ad^{n-2} \qquad \ldots\ldots\ldots \quad (8.4)$$

or,

$$H = aP^{\frac{n-2}{n}} \qquad \ldots\ldots\ldots \quad (8.5)$$

In case of Vickers microhardness, the value of exponent 'n' equals 2 (Kick's law 1885) for all indenters that give impressions geometrically similar to one another, Thus, n = 2 implies that hardness for a given shape of pyramidal indenter is constant and independent of load. In order to appreciate the detailed physical meaning of the above equations it will be instructive to consider the example of a solid subjected to a uniaxial compression. For such a simple case, the modulus of elasticity (Young's modulus) is given by

$$E = \frac{\sigma}{\epsilon} \qquad \ldots\ldots\ldots \quad (8.6)$$

where σ is the compressive stress defined as load per unit area

$$\sigma = \frac{P}{A} \qquad \ldots\ldots\ldots \quad (8.7)$$

and the compressive strain ϵ is defined as the decrease in length per unit length. Now the area of cross-section, A, increases with compression. Hence for a constant volume of a solid, length is inversely proportional to the area of cross-section. If A_o represents initial area of cross-section with a normal length l_o, and A the final area with normal length l after small compression, one obtains,

$$l A = l_o A_o$$

or

$$\frac{l}{l_o} = \frac{A_o}{A} \quad \text{........} \quad (8.8)$$

Therefore

$$\epsilon = \frac{l - l_o}{l} = \frac{A_o - A}{A} \quad \text{.........} \quad (8.9)$$

substitution of σ and ϵ from equations (8.7) and (8.9) gives

$$E = \frac{\sigma}{\epsilon} = \frac{P}{A_o - A} \quad \text{.........} \quad (8.10)$$

Hence for a simple uniaxial compressive stress when the area is a geometrical function of the deformation, determined here by constant volume, the resistance to permanent deformation can be expressed simply in terms of load and corresponding area. In indentation hardness work the volume change is very very small. Hence the indentation hardness can be measured by using above formula (Eq. 8.10). Indenters are made in various geometrical shapes such as spheres, pyramids etc. The area over which the force due to load on indenter acts increases with the depth of penetration. The resistance to permanent deformation or hardness can be expressed in terms of force or load and area alone (and/or depth of penetration). These remarks are true for solids which are amorphous or highly homogeneous and isotropic.

The above analysis presents a highly simplified picture of the process involved because there is a great difference between deforming a solid in a simple uniaxial compression and deforming a surface of a solid by pressing a small indenter into it. Around the indentation mark, the stress distribution is exceedingly complex and the stressed material is under the influence of multiaxial stresses. The sharp corners of a pyramidal indenter produces a sizable amount of plastic deformation which may reach 30% or more at the top of the indenter. Further the surface of contact is inclined by varying amounts to the directions of applied force. In view of these complications a simple expression corresponding to that for the modulus of elasticity can not be derived for hardness. In the absence of any formula based on sound theory, an arbitary expression is used which includes both known variables - load and area - in the present case. Hence the hardness number, H, is defined as the ratio of the load to the area of impression,

$$H = \frac{P}{A} \qquad \ldots\ldots\ldots \quad (8.11)$$

For pyramidal indenters the load (P) varies as the square of the diagonal, d. Thus for a given shape of pyramid,

$$P = bd^2 \qquad \ldots\ldots\ldots \quad (8.12)$$

where b is constant which depends on the material and shape of pyramid. The area of the impression, A, is also aproportional to the square of the diagonal,

$$A = cd^2 \qquad \ldots\ldots\ldots \quad (8.13)$$

where c depends upon the shape of the pyramid. Combination of equations 8.5, 8.6 and 8.7 gives

$$H = \frac{bd^2}{cd^2} = \frac{b}{c} = \text{Constant} \ldots \quad (8.14)$$

Hence for a given shape of pyramidal indenter hardness is independent of load and size of indentation. This statement represents Kick's law. In view of defining equation (8.5) for hardness, hardness number can also be considered as hardening modulus.

Due to complicated behaviour of indented isotropic single crystals of various materials and as a result of the development of arbitrary expression for hardness, it is clear that the theoretical treatment of the problem is extremely difficult. Hence it is desirable to approach this problem via experimental observations, interpretations and with a probable development of empirical relation(s). The present work is taken up from this phenomenological point of view and is an extension of the work carried out by Saraf (1971), Mehta (1972), Shah (1976) and Acharya (1978) in this laboratory.

8.2 OBSERVATIONS :

The observations which were recorded for studying the equation $P = ad^n$ are used in the present investigation (Table 8.1 and 8.2). The Knoop and Vickers hardness numbers are calculated using equation (8.1) and (8.2) for thermally treated and untreated samples. The observations are graphically studied by plotting the graphs of hardness number versus load P (Fig. 8.1, 8.2, 8.3, 8.4 and 8.5). In what follows the hardness and hardness number will be used to indicate same meaning.

8.3 RESULTS AND DISCUSSION :

It is clear from the graphs of hardness number (H) versus load (P) that contrary to theoretical expectations, the hardness varies with load. The hardness at first increases with load, reaches a maximum value then gradually

TABLE - 8.1 (KNOOP INDENTER)

LOAD P in gm.	Hk (Kg. mm^{-2})				
	$303^{\circ}k$	$573^{\circ}k$	$623^{\circ}k$	$673^{\circ}k$	$77.3^{\circ}k$
2.5	62.04	56.02	62.07	34.01	44.92
3.75	67.19	65.00	69.94	80.16	63.10
5.0	68.01	80.01	71.70	68.02	82.30
7.5	99.47	92.21	96.94	94.53	105.74
8.75	103.58	103.05	107.20	102.16	123.90
10	89.36	99.59	104.17	114.32	132.59
12.5	111.70	114.11	124.48	133.22	124.48
15	120.95	131.29	131.29	134.07	121.00
20	115.83	113.26	124.25	113.26	92.59
30	116.68	92.21	107.55	118.34	84.73
40	101.74	92.27	109.76	95.31	106.57
50	91.46	95.61	99.83	106.07	96.92
60	95.62	106.74	102.78	105.68	100.91
70	93.31	94.07	99.61	106.74	112.50
80	90.52	90.52	99.25	110.19	99.24
100	89.04	92.54	99.32	102.17	99.36
120	89.93	91.64	91.64	97.54	107.55
140	88.50	92.66	93.79	106.29	98.85
160	90.33	80.66	101.32	104.07	105.36

TABLE - 8.2 (VICKERS INDENTER)

LOAD P in gm.	Hv (Kg. mm^{-2})				
	303°k	573°k	623°k	673°k	773°k
2.5	49.68	55.73	64.00	72.01	64.00
3.75	78.85	66.05	69.52	97.02	69.52
5.0	72.08	76.61	82.50	84.12	84.08
7.5	87.64	84.21	84.21	82.01	84.73
8.75	88.75	80.91	87.32	91.84	92.96
10.0	85.84	89.41	94.45	96.51	94.59
12.5	95.96	90.53	100.17	105.94	102.86
15	93.78	88.67	102.15	110.69	103.39
20	91.23	101.64	102.71	106.95	103.69
30	104.23	101.58	96.48	93.73	96.48
40	88.30	94.59	100.98	99.50	101.73
50	88.31	91.67	92.77	93.42	92.83
60	78.60	88.27	90.29	91.53	90.81
70	85.35	90.83	90.78	90.82	90.87
80	79.29	87.04	91.78	93.16	92.24
100	78.05	83.43	85.71	86.86	85.85
120	79.35	78.02	-	87.06	-
140	77.27	84.75	85.80	-	85.77
160	70.91	81.47	82.10	85.79	82.37

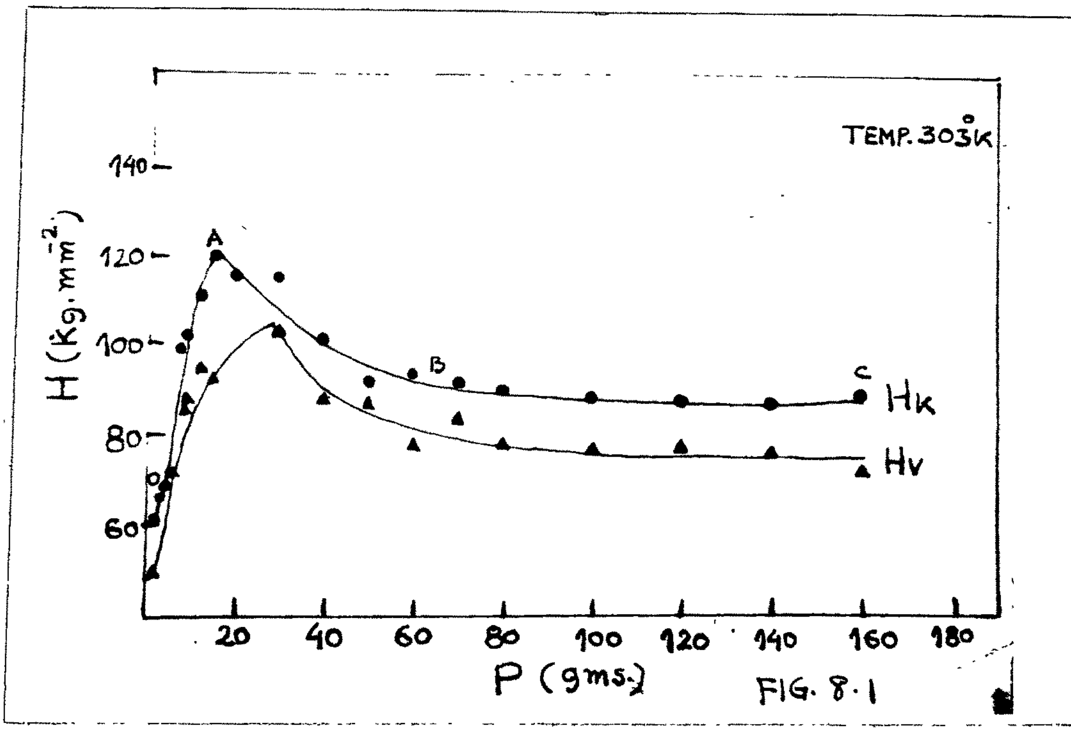

Fig. 8.1 Plot of Hardness number(H) versus load P for temperature 303°K.

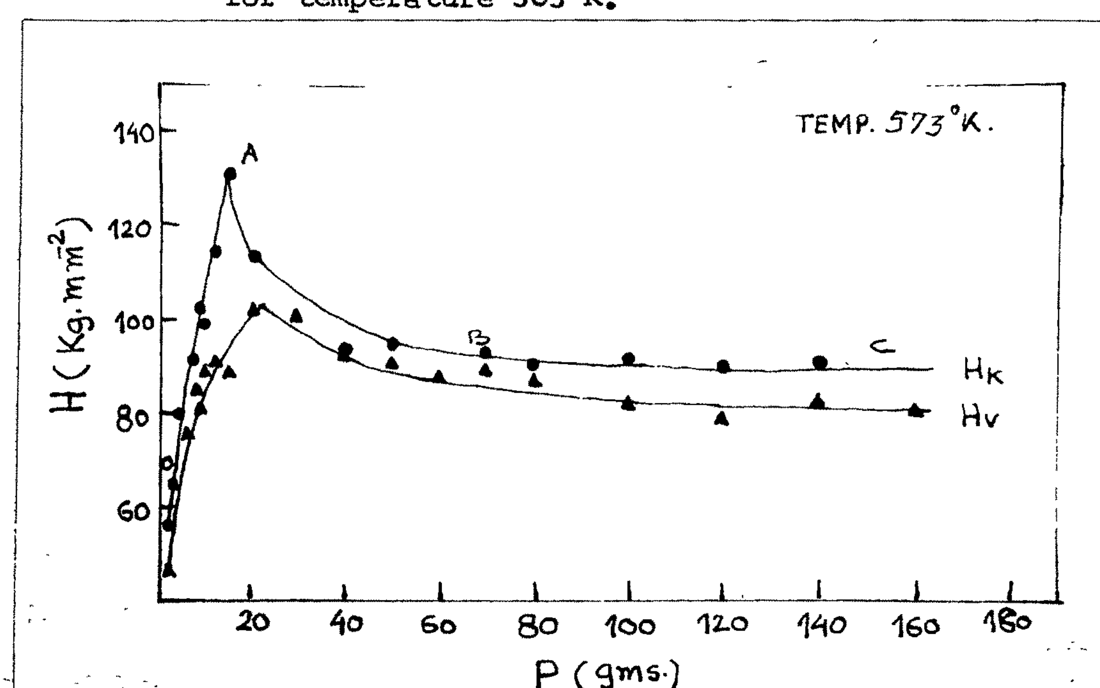

Fig. 8.2 Plot of Hardness number(H) versus load P for quenching temperature 573°K.

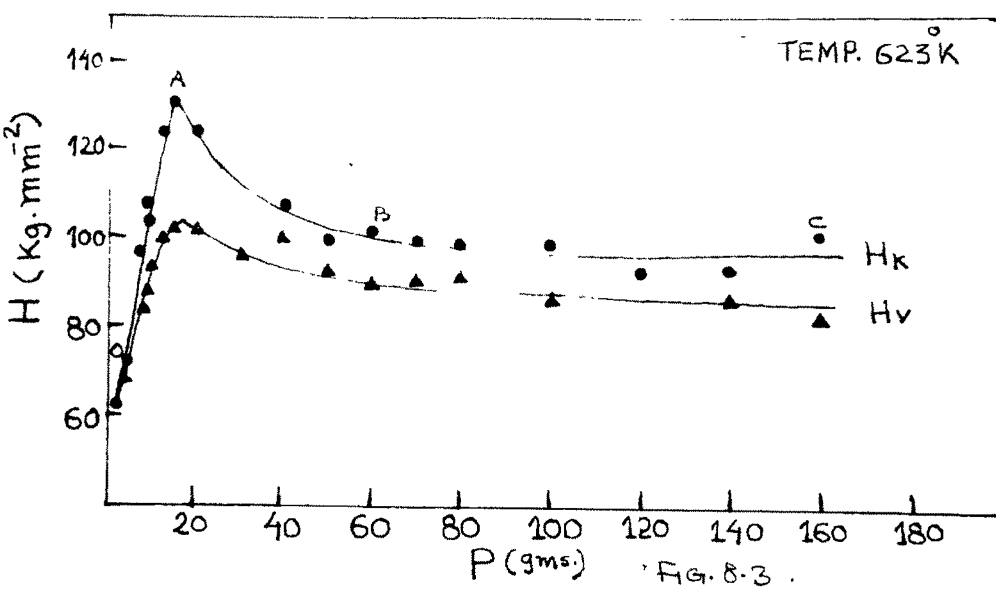

Fig. 8.3 Plot of Hardness number(H) versus load P for quenching temperature 623°K

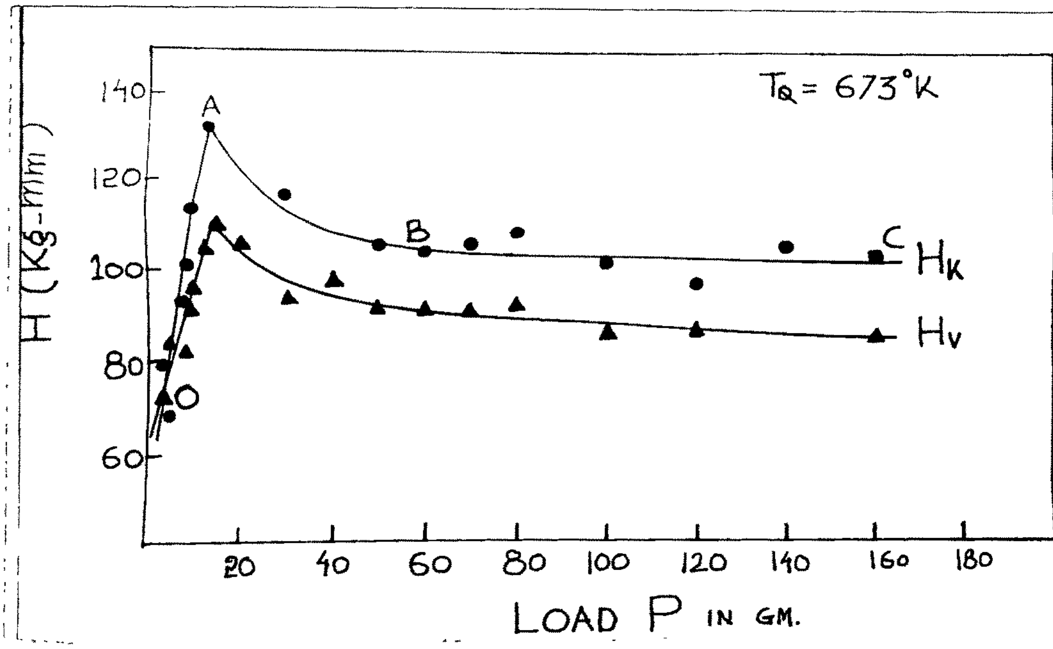

Fig. 8.4 Plot of Hardness number(H) versus load P for quenching temperature 673°K

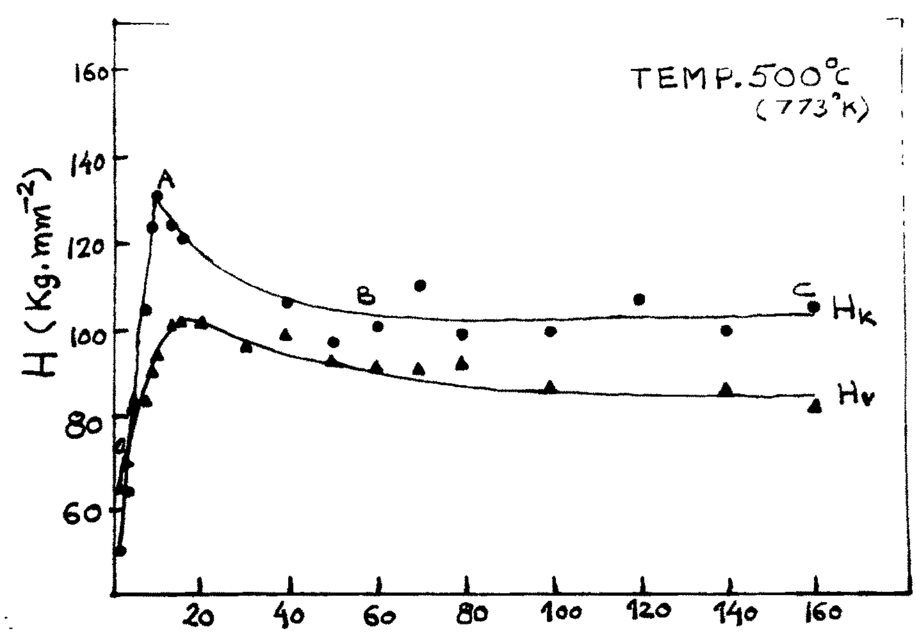

Fig. 8.5 Plot of Hardness number(H) versus load P for quenching temperature 773^{O}K.

decreases, and attains a constant value for all loads. This behaviour is found for both types of hardness numbers viz. Knoop hardness number (H_k) and Vickers hardness number (H_v). Further, Knoop hardness number (H_k) has higher values than Vickers hardness number (H_v) for all loads and for all samples irrespective of heat treatment. The theoretical conclusion that hardness is independent of load thus appears to be true only at higher loads. The maximum value of hardness corresponds with a load which is nearer the value of the load at which kink in the graph of log P versus log d is observed (cf, Chapter-7). The graph of H versus P can be conveniently divided into three parts OA, AB and BC where the first part represents linear relation between hardness and load, the second part, the non-linear relation and the third part the linear one. It should be noted that there is a fundamental difference between linear portions OA and BC of the graph OABC. This possibly reflects varied reactions of the cleavage surface to loads belonging to different regions. Besides it supports, to a certain extent, the earlier view about the splitting of the graph of log P versus log d into two recognizable lines (cf, Chapter-7).

The qualitatively complex behaviour of microhardness with load can be explained on the basis of the depth of penetration of the indenter. At small loads the indenter penetrates only surface layers, hence the effect is shown more sharply at these loads. However, as the depth of the impression increases, the effect of surface layers becomes less dominant and after a certain depth of penetration, the effect of inner layers becomes more and more prominent than those of surface layers and ultimately there is practically no change in value of hardness with load. It is also clear from the graphs that the Knoop hardness number at lower loads increases rapidly with load as compared with the change in Vickers hardness number with load in identical load region. Since the Knoop hardness number, H_k, in general measures the hardness of surface layers, the above explanation based on the depth of penetration is quite logical.

8.3.1 <u>Relation between hardness and quenching temperature</u> :

It is clear from the observations of hardness of quenched and unquenched samples (Tables 8.1 and 8.2) that hardness depends upon the quenching temperature (T_Q). Hardness in high load region (HLR) is independent of load. Hence average values of hardness ($\bar{H}$) in high load region are computed and are recorded in Table 8.3. Fig. 8.6 shows the plot of log ($\bar{H}$ T_Q) versus log T_Q. The plot is a straight line for Knoop as well as Vickers hardness numbers. Further, both the straight lines are parallel to each other having a

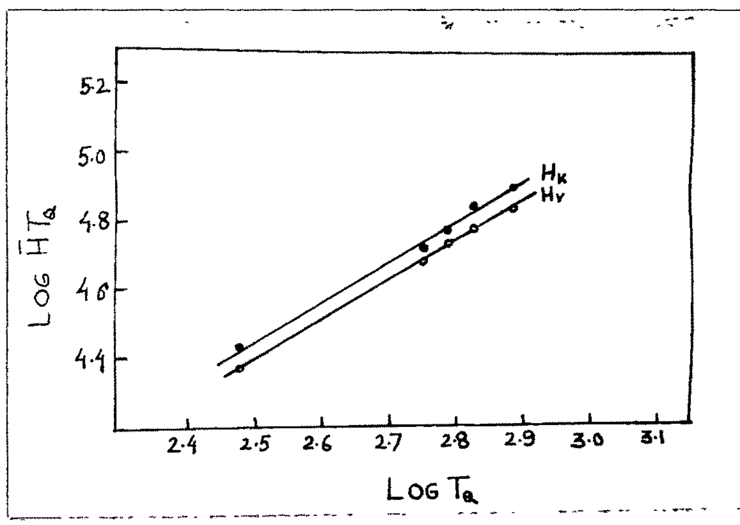

Fig. 8.6 Plot of log ($\bar{H}T_Q$) versus log T_Q (HLR)

TABLE - 8.3 (HLR)

Quenching Temperature T_Q °K	log T_Q	$\overline{H}_k$ Kg. mm^{-2}	$\overline{H}_v$ Kg. mm^{-2}	log $\overline{H}_k T_Q$	log $\overline{H}_v T_Q$	$\frac{\overline{H}_k}{\overline{H}_v}$	Mean $\frac{\overline{H}_k}{\overline{H}_v}$
303	2.4814	91.09	79.64	4.4409	4.3825	1.14	
573	2.7582	92.99	85.68	4.7266	4.6910	1.08	
623	2.7944	98.44	88.46	4.7876	4.7412	1.11	1.13
673	2.8280	104.84	89.71	4.8485	4.7808	1.17	
773	2.8882	102.58	88.69	4.8992	4.8360	1.16	

TABLE 8.4 (HLR)

Quenching Temperature T_Q ^oK	C_k (By Calc)	C_v (By Calc)	% deviation of C_k from mean C_k	% deviation of C_k from value of C_k (graph)	% deviation of C_v from mean C_v	% deviation of C_v from value of C_v (graph)
303	45.89	40.12	0.2	0.02	0.67	0.00
573	43.39	39.97	5.2	5.47	1.04	0.37
623	45.49	40.87	6.5	0.89	0.01	1.87
673	47.99	41.07	4.8	4.55	1.68	2.37
773	46.18	39.92	0.8	0.61	1.16	0.50
Mean	45.788	40.39	-	-	-	-
Values from graph	45.90	40.12	-	-	-	-

constant slope and different intercepts on log ($\bar{\bar{H}}$ T_Q) axis. The straight line graph follows the equation,

$$\log \bar{H}\, T_Q = m \log T_Q + \log C \quad \ldots\ldots\ldots \quad (8.15)$$

where m is the slope and C is a constant. Therefore,

$$\bar{H}\, T_Q^{\,1-m} = C \quad \ldots\ldots\ldots \quad (8.16)$$

or,

$$\bar{H}\, T_Q^{\,k} = C \quad \ldots\ldots\ldots \quad (8.17)$$

where $k = 1 - m$. The value of k is -0.12 for calcite.

It is clear from table 8.3 that quantitatively knoop hardness number is 1.13 times the vickers hardness number of calcite cleavage faces in the HLR region. Further for both indenters, the hardness number increases with quenching temperature. However the percentage increase in hardness with respect to hardness at room temperature ($303^{\circ}K$) is quite small. This percentage changes for Knoop hardness and vickers hardness are respectively 12.6% and 11.4% and their ratio is 1.1 which corresponds approximately to the ratio $\bar{H}_k : \bar{H}_v$ (Table 8.3).

It is desirable to ascertain how far the relation $\bar{H}\, T_Q^{\,k}$ = constant is true for individual observations on quench hardness. This constant is designated by C and the subscript K and V indicates respectively the use of Knoop and Vickers indenters for obtaining the Hardness values (Table 8.4). The percentage changes in hardness values from its mean value are small. Further the comparision indicates that the percentage changes for Knoop hardness number are greater than those of Vickers hardness number. The author had consistently tried to find the reason for these large deviations by repeating the work several times. However the results were not significantly different from the present ones. The reasons are unknown for such a large deviation. Since Knoop indenter is normally used for studying crystalline anisotropy, the relatively large deviation is likely to be associated with the inherent utility of the indenter. At present there is no experimental evidence to support it. From the empirical formulae for Knoop and Vickers hardness numbers it is obvious that hardness number is inversely proportional to square of the diagonal of the indentation mark for a constant load. Since hardness depends on temperature of quenching, the diagonal length of the indentation mark would also depend on the quenching temperature. Thus for both the indenters

$$H = R \cdot \frac{P}{d^2} \qquad \text{........ (8.18)}$$

where R is a constant depending upon the geometry of the indenter. Further,

$$HT_Q^{\,k} = C \qquad \ldots\ldots\ldots\ldots \quad (8.19)$$

Combination of above equations gives,

$$\frac{PT_Q^{\,k}}{d^2} = \frac{C}{R} = \text{Constant} = S \quad \ldots. \quad (8.20)$$

or $$\frac{T_Q}{d^2} \times PT_Q^{\,k-1} = S \quad \ldots\ldots\ldots \quad (8.21)$$

$$\frac{T_Q}{d^2} = \frac{S}{P} \; T_Q^{\,1-k} \qquad \ldots\ldots\ldots\ldots \quad (8.21)$$

or $$\log \frac{T_Q}{d^2} = \log \left(\frac{S}{P}\right) + (1-k) \log T_Q$$

or $$\log \frac{T_Q}{d^2} = (1-k) \log T_Q + \log S - \log P$$

$$\ldots\ldots \quad (8.22)$$

or $$\log \frac{T_Q}{d^2} = m_1 \log T_Q + \log A \quad \ldots\ldots \quad (8.23)$$

On simplifying it one gets (using eg. 8.20)

$$\frac{T_Q^{\,1-m_1}}{d^2} = A = \frac{S}{P} = \frac{C}{RP} \quad \ldots. (8.24a)$$

$$\text{or} \quad \frac{T_Q^{\,k}}{d^2} = \frac{C}{RP} = A \qquad \text{........} \quad (8.24b)$$

It is obvious from the above equation that for a given applied load if a graph of log (T_Q/d^2) is plotted against log T_Q, the slope of the graph will be $(1 - k)$. However if this is repeated for several applied loads, it is evident from above equation that graph of log (T_Q/d^2) versus log T_Q should consist of straight lines parallel to one another having slope $(1 - k)$ and different intercepts.

It is possible to find out the spacing between two parallel lines. Thus for the applied loads P_1 and P_2

$$\log \frac{T_{Q1}}{d_1^{\,2}} = (1 - k) \log T_{Q1} + \log S - \log P_1$$

$$\log \frac{T_{Q2}}{d_2^{\,2}} = (1 - k) \log T_{Q2} + \log S - \log P_2$$

The difference in above two equations is

$$\log \frac{T_{Q1}}{d_1^{\,2}} - \log \frac{T_{Q2}}{d_2^{\,2}} = (1 - k) \log \frac{T_{Q1}}{T_{Q2}} + \log \frac{P_2}{P_1}$$

or

$$\log \frac{T_{Q1}\ d_2^{\ 2}}{T_{Q2}\ d_1^{\ 2}} = (1 - k) \log \frac{T_{Q1}}{T_{Q2}} + \log \frac{P_2}{P_1}$$

In terms of A_1 and A_2 the above equation becomes

$$\log \frac{T_{Q1}\ d_2^{\ 2}}{T_{Q2}\ d_1^{\ 2}} = m_1 \log \frac{T_{Q1}}{T_{Q2}} - \log \frac{A_2}{A_1}$$

These equations are fully reflected by the graphical plotts of log $(T_Q/d_k^{\ 2})$ versus log T_Q (Fig. 8.7, Table 8.5) and log $(T_Q/d_v^{\ 2})$ versus log T_Q (Fig. 8.8, Table 8.6). They provide results which are in agreement with above conclusions, Further, the slope of any one plot (Fig. 8.7 and 8.8) is 1.12.

$$\text{i.e.} \quad 1 - k = m_1 = 1.12$$

Hence the value of k is -0.12 which is identical with the value of the exponent k in the equation 8.19 connecting hardness number and quenching temperature.

In Chapter - 7 the variation of applied load with diagonal of an indentation mark was studied by critically examining empirical formula, known as Kick's law.

$$P = ad^n \qquad \text{..........} \quad (8.25)$$

TABLE - 8.5 (KNOOP INDENTER)

LOAD P in gm.	Log (T_O/ dk^2)				
	$303^\circ k$	$573^\circ k$	$623^\circ k$	$673^\circ k$	$773^\circ k$
30	$\bar{2}.9180$	$\bar{1}.0927$	$\bar{1}.1956$	$\bar{1}.2709$	$\bar{1}.1856$
40	$\bar{2}.7340$	$\bar{2}.9680$	$\bar{1}.0795$	$\bar{1}.0519$	$\bar{1}.1606$
50	$\bar{2}.5904$	$\bar{2}.8075$	$\bar{2}.9415$	$\bar{1}.0013$	$\bar{1}.0224$
60	$\bar{2}.5302$	$\bar{2}.7882$	$\bar{2}.8751$	$\bar{2}.9206$	$\bar{2}.9605$
70	$\bar{2}.4533$	$\bar{2}.7332$	$\bar{2}.7731$	$\bar{2}.8579$	$\bar{2}.9410$
80	$\bar{2}.3820$	$\bar{2}.6590$	$\bar{2}.7348$	$\bar{2}.8136$	$\bar{2}.8287$
100	$\bar{2}.2765$	$\bar{2}.5694$	$\bar{2}.6385$	$\bar{2}.6839$	$\bar{2}.7316$
120	$\bar{2}.2014$	$\bar{2}.4871$	$\bar{2}.5237$	$\bar{2}.5843$	$\bar{2}.6875$
140	$\bar{2}.1271$	$\bar{2}.4232$	$\bar{2}.4669$	$\bar{2}.5551$	$\bar{2}.5832$
160	$\bar{2}.0792$	$\bar{2}.3075$	$\bar{2}.4425$	$\bar{2}.4871$	$\bar{2}.5539$

TABLE - 8.6 (VICKERS INDENTER)

LOAD P In gm.	Log (T_Q / d_V^2)				
	303°k	573°k	623°k	673°k	773°k
30	$\bar{1}.7542$	0.0197	0.0337	$\bar{1}.9557$	0.1274
40	$\bar{1}.5578$	$\bar{1}.8638$	$\bar{1}.9286$	$\bar{1}.8309$	0.0254
50	$\bar{1}.4620$	$\bar{1}.7533$	$\bar{1}.7948$	$\bar{1}.7433$	$\bar{1}.8888$
60	$\bar{1}.3265$	$\bar{1}.6577$	$\bar{1}.7038$	$\bar{1}.6728$	$\bar{1}.8000$
70	$\bar{1}.2980$	$\bar{1}.6031$	$\bar{1}.6393$	$\bar{1}.6258$	$\bar{1}.7334$
80	$\bar{1}.2092$	$\bar{1}.5266$	$\bar{1}.5861$	$\bar{1}.4986$	$\bar{1}.6818$
100	$\bar{1}.1059$	$\bar{1}.4113$	$\bar{1}.4594$	$\bar{1}.3536$	$\bar{1}.5538$
120	$\bar{1}.0342$	$\bar{1}.3029$	-	$\bar{1}.2887$	-
140	$\bar{2}.9552$	$\bar{1}.2720$	$\bar{1}.3137$	-	$\bar{1}.4072$
160	$\bar{2}.8597$	$\bar{1}.1970$	$\bar{1}.2365$	$\bar{1}.2697$	$\bar{1}.3316$

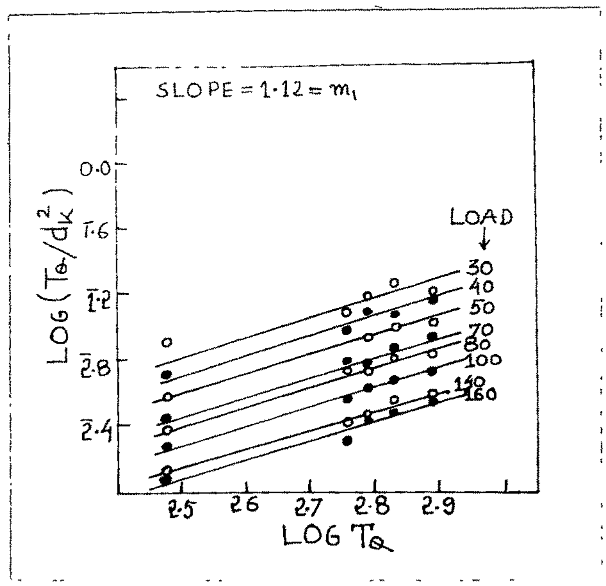

Fig. 8.7 Plot of log (T_Q/d_k^2) versus log T_Q for various loads (HLR)

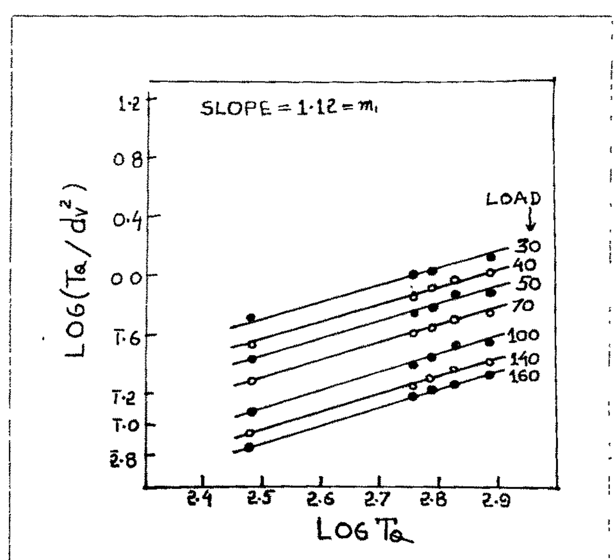

Fig. 8.8 Plot of log (T_Q/d_v^2) versus log T_Q for various loads (HLR)

TABLE - 8.7 (KNOOP INDENTER)

LOAD P in gm.	Log ($a_2\, d_k^{\,2} / T_Q$)				
	$303^\circ k$	$573^\circ k$	$623^\circ k$	$673^\circ k$	$773^\circ k$
30	$\bar{1}.3296$	$\bar{1}.1552$	$\bar{1}.0640$	$\bar{1}.0254$	$\bar{1}.0733$
40	$\bar{1}.5136$	$\bar{1}.2800$	$\bar{1}.1801$	$\bar{1}.2444$	$\bar{1}.0986$
50	$\bar{1}.6572$	$\bar{1}.4406$	$\bar{1}.3182$	$\bar{1}.2949$	$\bar{1}.2367$
60	$\bar{1}.7172$	$\bar{1}.4596$	$\bar{1}.3847$	$\bar{1}.3756$	$\bar{1}.2984$
70	$\bar{1}.7947$	$\bar{1}.5146$	$\bar{1}.4866$	$\bar{1}.4382$	$\bar{1}.3$[illegible]80
80	$\bar{1}.8659$	$\bar{1}.5892$	$\bar{1}.5248$	$\bar{1}.4824$	$\bar{1}.4305$
100	$\bar{1}.9700$	$\bar{1}.6788$	$\bar{1}.6215$	$\bar{1}.6122$	$\bar{1}.5272$
120	0.0446	$\bar{1}.7600$	$\bar{1}.7356$	$\bar{1}.7114$	$\bar{1}.5718$
140	0.1182	$\bar{1}.8244$	$\bar{1}.7924$	$\bar{1}.7412$	$\bar{1}.6753$
160	0.1678	$\bar{1}.9404$	$\bar{1}.8169$	$\bar{1}.8083$	$\bar{1}.7056$

TABLE - 8.8 (VICKERS INDENTER)

LOAD P in gm.	Log ($a_2 d_v^2 / T_Q$)				
	303^oK	573^oK	623^oK	673^oK	773^oK
30	$\bar{1}.2457$	$\bar{2}.9789$	$\bar{2}.9782$	$\bar{2}.9691$	$\bar{2}.8975$
40	$\bar{1}.4621$	$\bar{1}.1648$	$\bar{1}.0833$	$\bar{1}.1520$	$\bar{2}.9997$
50	$\bar{1}.5097$	$\bar{1}.2553$	$\bar{1}.2171$	$\bar{1}.1930$	$\bar{2}.1951$
60	$\bar{1}.6735$	$\bar{1}.3409$	$\bar{1}.3081$	$\bar{1}.2805$	$\bar{1}.2247$
70	$\bar{1}.7019$	$\bar{1}.3955$	$\bar{1}.3726$	$\bar{1}.3511$	$\bar{1}.2914$
80	$\bar{1}.7907$	$\bar{1}.4719$	$\bar{1}.4259$	$\bar{1}.3980$	$\bar{1}.3420$
100	$\bar{1}.8939$	$\bar{1}.5873$	$\bar{1}.5525$	$\bar{1}.5253$	$\bar{1}.4711$
120	$\bar{1}.9657$	$\bar{1}.6955$	-	$\bar{1}.6702$	-
140	0.0447	$\bar{1}.7265$	$\bar{1}.6981$	-	$\bar{1}.6175$
160	0.1400	$\bar{1}.8017$	$\bar{1}.7753$	$\bar{1}.7347$	$\bar{1}.6931$

It was shown that a and n are constants and the straight line represented by the plot of log $\frac{P}{d}$ versus log d consists of two straight lines with slopes n_1 and n_2 and intercepts a_1 and a_2 respectively. The slope n_2 and the intercept a_2 approximately correspond to HLR region of the graph of hardness versus load. (Fig. 8.1, 8.2, 8.3, 8.4 and 8.5). The combination of equations 8.20 and 8.25 yields,

$$\frac{a_2 d^{n_2} T_Q^{k}}{d^2} = S \quad \ldots\ldots\ldots \quad (8.26)$$

Substituting

$$d^2 = P / a_2 d^{n_2 - 2}$$

in eqn.8.24a, one gets

$$\frac{T_Q^{1 - m_1}}{P} \times a_2 d^{n_2 - 2} = A \quad \ldots\ldots \quad (8.27)$$

Since n_2 is not having an integral value, it is necessary to have a different approach. If graphs of log $(a_2 d_k^{\,2}/T_Q)$ versus log T_Q and log $(a_2 d_v^{\,2}/T_Q)$ versus log T_Q are plotted, they consist of a series of parallel lines corresponding to different intercepts (Fig. 8.9 and 8.10). Thus each straight line follows the general equation.

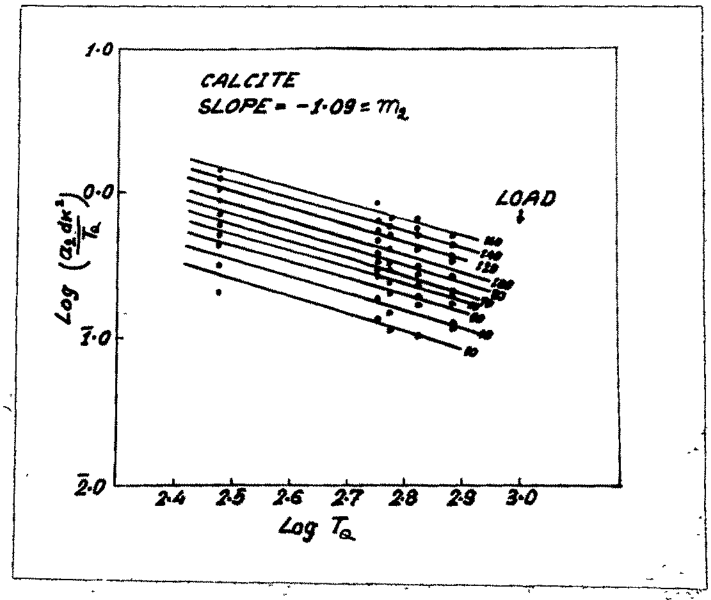

Fig. 8.9 Plot of log $(a_2 d_k{}^2/T_Q)$ versus log T_Q for various loads (HLR)

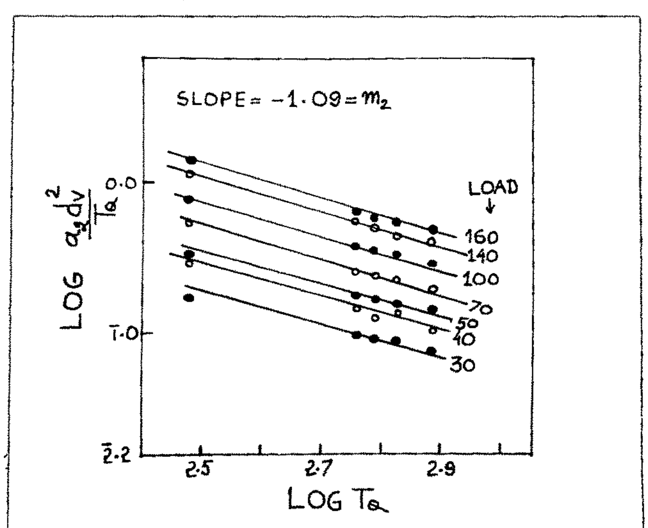

Fig. 8.10 Plot of log $(a_2 d_v{}^2/T_Q)$ versus log T_Q for various loads (HLR)

$$\log \frac{a_2 d^2}{T_Q} = m_2 \log T_Q + \log B \qquad \text{........ (8.28)}$$

Slope of each straight line is $m_2 = -1.09$. Simplification of the above equation yields

$$a_2 d^2 T_Q^{0.09} = B \qquad \text{........ (8.29)}$$

Combining above equation with eqn.8.25 one obtains

$$P d^{2-n_2} T_Q^{0.09} = B \qquad \text{........ (8.30)}$$

Comparision of Kick's law (Eq. 8.25) with formulae for hardness numbers (Eq. 8.1 and 8.2) clearly suggest that the constant a and hardness numbers are related. Inspection of the variation of various functions involving H, a_2 and T_Q has disclosed that the graph of log ($\bar{H}T_Q$ / a_2) versus log T_Q would be a straight line, (Fig. 8.11, Table 8.9) following the equation,

$$\log \frac{\bar{H}T_Q}{a_2} = m_3 \log T_Q + \log E \qquad \text{........ (8.31)}$$

where slope is given by $m_3 = 1.09$ and E is a constant. These plots for Knoop and Vickers hardness numbers are presented in Fig. 8.11 (Table 8.9)

TABLE 8.9 (HLR)

Temperature T_Q ^oK	$\log \overline{H}_k$	$\log \overline{H}_v$	$\log a_2\overline{H}_k$	$\log a_2\overline{H}_v$	$\log \frac{\overline{H}_k T_Q}{a_2}$	$\log \frac{\overline{H}_v T_Q}{a_2}$	$\log T_Q$
303	1.9595	1.9011	0.2074	0.9011	6.1929	5.3825	2.4814
573	1.9684	1.9328	0.2164	0.9328	6.4786	5.6910	2.7582
623	1.9932	1.9467	0.2532	0.9596	6.5276	5.7284	2.7944
673	2.0205	1.9528	0.2947	0.9781	6.5744	5.7555	2.8280
773	2.0111	1.9479	0.2711	0.9732	6.6392	5.8107	2.8882

substituting $a_2 = \frac{P}{d^2} d^{2 - n_2}$ and

$H = \frac{R \; P}{d^2}$ in eq. 8.31,

one gets

$$E = RT_Q^{1 - m_3} \quad d^{n_2 - 2} \qquad \ldots\ldots\ (8.32)$$

Simplifying eq. 8.31 gets

$$\frac{\bar{H} \; T_Q^{1 - m_3}}{a_2} = E \qquad \ldots\ldots\ldots\ (8.33)$$

i.e. $$\frac{\bar{H} \; T_Q^{-0.09}}{a_2} = E \qquad \ldots\ldots\ldots\ (8.34)$$

Multiplication of eq. (8.27) with eq. (8.30) gives

$$T_Q^{k} \cdot a_2 \; d^{n_2 - 2} \cdot Pd^{2 - n_2} \cdot T_Q^{0.09} = AB$$

or $$a_2 T_Q^{(k + 0.09)} = AB = \text{Constant} \;\ldots.\ (8.35)$$

Thus the intercepts a_2 could be associated with the quenching temperature. This can also be understood from a graphical plot of log $(a_2 T_Q)$ versus log T_Q which follows the equation

$$\log (a_2 T_Q) = m_4 \log T_Q + \log D \qquad \ldots\ldots\ (8.36)$$

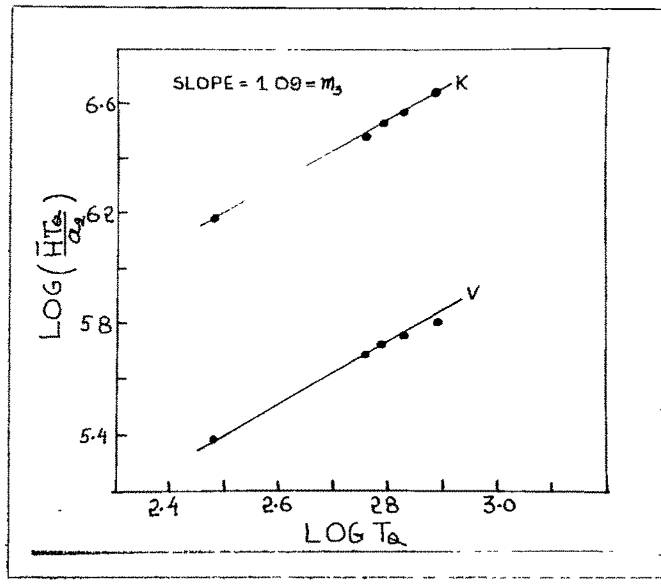

Fig. 8.11 Plot of log ($\bar{H}$ T_Q/a_2) versus log T_Q

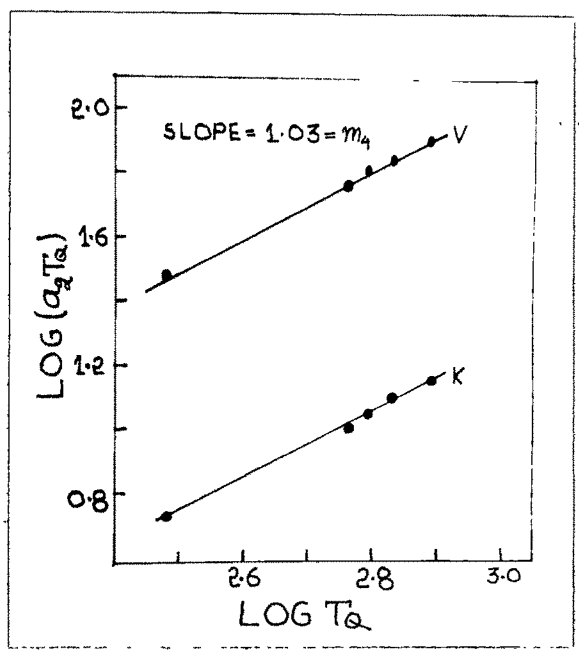

Fig. 8.12 Plot of log (a_2T_Q) versus log T_Q

The graphs of log (a_2T_Q) versus log T_Q for Knoop and Vickers indenters are shown in figure 8.12. (Table 7.3 and 7.2). Thus,

$$a_2 T_Q^{1 - m_4} = D \qquad \ldots\ldots\ (8.37)$$

where m_4 is the slope of fig. 8.12 and equals 1.03. Hence the above equation becomes

$$a_2 T_Q^{-0.03} = D \qquad \ldots\ldots\ (8.38)$$

substituting

$$a_2 = \frac{P}{d^2} \cdot d^{2 - n_2} \quad \text{in eq. (8.37)}$$

one gets

$$\frac{P}{d^2} \; d^{2 - n_2} \; T_Q^{1 - m_4} = D \qquad \ldots\ldots\ (8.39)$$

Slight dependence of a_2 on quenching temperature can be expected because value of a_2 is (Tables 7.3 and 7.2) quite small. It is suggested from the form of equations 8.25 and 8.18 that there must be some relation between hardness number and a_2. After considering several functions containing H and a_2 it was found that the plots of log (a_2H_k) versus log H_k and log $(a_2\ H_v)$ versus log H_v give a better straight line, obeying the general equation

$$\log (a_2\bar{H}) = m_5 \log \bar{H} + \log F \quad \ldots\ldots\ldots (8.40)$$

on Simplification one gets

$$a_2\bar{H}^{1 - m_5} = F \quad \ldots\ldots\ldots (8.41)$$

Slope of the above plot (fig. 8.13 and 8.14) is given by $m_5 = 1.25$. Hence the above equation becomes

$$a_2\bar{H}^{-0.25} = F \quad \ldots\ldots\ldots (8.42)$$

This shows very clearly that hardness number and the intercept of the straight line (cf,fig. 8.13 and 8.14) corresponding to HLR are intimately connected.

It is thus clear from above equations that Kick's law and formulae for hardness numbers are intimately connected in the HLR region of the graph of hardness member versus applied load.

It is interesting to examine the accuracy of each observation in the above plots by considering the coefficient of variation for different constants associated with different equations mentioned above.

The values of A, B, E, and D are computed for each observation using equations 8.27, 8.29, 8.32 and 8.39

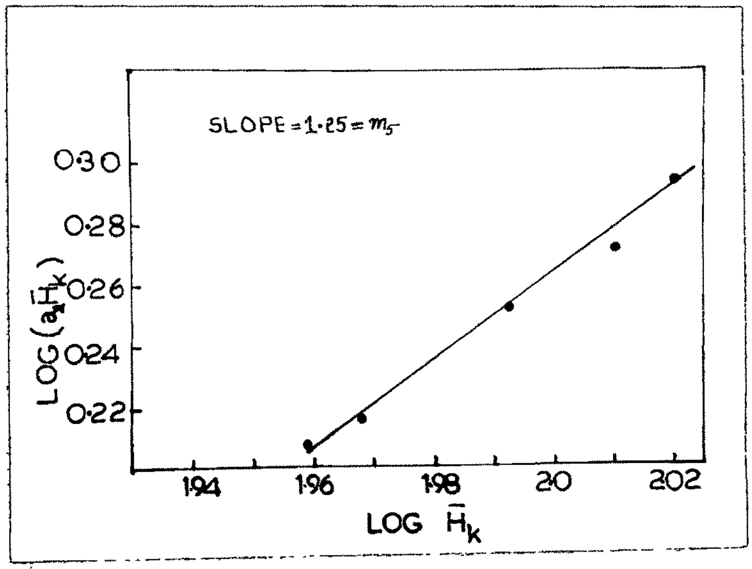

Fig. 8.13 Plot of log $(a_2\bar{H}_k)$ versus log $\bar{H}_k$

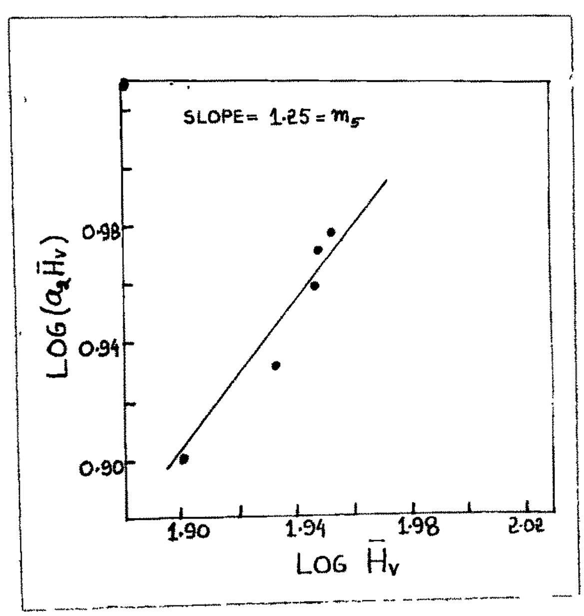

Fig. 8.14 Plot of log $(a_2\bar{H}_v)$ versus log $\bar{H}_v$

respectively and are presented in Tables 8.10.1 to 8.10.10. For these tables the above equations are collected here and are given in sequence with new equation numbers.

$$A = \frac{T_Q}{P}^{1 - m_1} \cdot a_2 d^{n_2 - 2} \qquad \ldots\ldots (8.43)$$

$$A_k = \frac{T_Q}{P}^{1 - m_1} \cdot a_{2k} d_k^{n_2 - 2} \qquad \ldots\ldots (8.43a)$$

$$A_v = \frac{T_Q}{P}^{1 - m_1} \cdot a_{2v} d_v^{n_2 - 2} \qquad \ldots\ldots (8.43b)$$

$$B = P\, d^{2 - n_2}\, T_Q^{0.09} \qquad \ldots\ldots\ldots\ldots (8.44)$$

$$B_k = P\, d_k^{2 - n_2}\, T_Q^{0.09} \qquad \ldots\ldots\ldots\ldots (8.44b)$$

$$B_v = P\, d_v^{2 - n_2}\, T_Q^{0.09} \qquad \ldots\ldots\ldots\ldots (8.44b)$$

$$\frac{P}{B} = \frac{d^{n_2 - 2}}{T_Q^{0.09}} \qquad \ldots\ldots\ldots\ldots (8.45)$$

$$\frac{P}{B_k} = \frac{d_k^{n_2 - 2}}{T_Q^{0.09}} \qquad \ldots\ldots\ldots\ldots (8.45a)$$

$$\frac{P}{B_v} = \frac{d_v^{n_2 - 2}}{T_Q^{0.09}} \qquad \ldots\ldots\ldots\ldots (8.45b)$$

TABLE 8.10.1 (KNOOP INDENTER)

QUENCHING TEMPERATURE $T_Q = 303^oK$

LOAD P in GM.	$A_k \times 10^{-4}$	$B_k \times 10^2$	$A_kB_k \times 10^{-2}$	$D_k \times 10^{-2}$	$\frac{P}{B_k} \times 10^{-2}$	$A_kP \times 10^{-2}$	$E_k \times 10^2$	$\frac{D_kE_k}{14230} \times 10^{-2}$
30	1.31	1.13	1.49	1.50	26.55	0.39	37.45	0.39
40	0.94	1.58	1.48	1.43	25.32	0.37	35.90	0.36
50	0.73	2.04	1.49	1.32	24.51	0.36	34.73	0.32
60	0.59	2.48	1.47	1.41	24.19	0.35	34.25	0.34
70	0.50	3.01	1.51	1.40	23.25	0.35	33.65	0.33
80	0.43	3.43	1.48	1.73	23.32	0.34	33.11	0.40
100	0.34	4.39	1.49	1.40	22.78	0.34	32.32	0.32
120	0.28	5.36	1.50	1.43	22.39	0.33	31.76	0.32
140	0.23	6.36	1.47	1.43	22.01	0.32	31.23	0.31
160	0.20	7.36	1.47	1.47	21.74	0.32	30.88	0.32
Mean	-	-	1.48	1.45	23.60	0.35	33.52	0.34

TABLE 8.10.2 (KNOOP INDENTER)

QUENCHING TEMPERATURE T_Q = $573^{o}K$

LOADPP IN GM.	$A_k \times 10^{-4}$	$B_k \times 10^{2}$	$A_k B_k \times 10^{-2}$	$D_k \times 10^{-2}$	$\frac{P}{B_k} \times 10^{-2}$	$A_k P \times 10^{-2}$	$E_k \times 10^{2}$	$\frac{D_k E_k}{14230} \times 10^{-2}$
30	1.20	1.24	1.49	1.25	24.19	0.36	34.56	0.30
40	0.86	1.70	1.47	1.28	23.53	0.34	33.58	0.30
50	0.65	2.21	1.44	1.15	22.63	0.32	32.37	0.26
60	0.55	2.66	1.46	1.32	22.55	0.33	32.23	0.30
70	0.47	3.15	1.48	1.38	22.22	0.33	31.82	0.31
80	0.40	3.66	1.46	1.35	21.86	0.32	31.28	0.30
100	0.31	4.67	1.45	1.40	21.41	0.31	30.64	0.30
120	0.26	5.71	1.48	1.42	21.01	0.31	30.08	0.30
140	0.22	6.76	1.49	1.45	20.71	0.31	29.63	0.29
160	0.18	7.93	1.43	1.30	20.18	0.29	28.84	0.26
Mean	-	-	1.47	1.33	22.03	0.32	31.50	0.29

TABLE 8.10.3 (KNOOP INDENTER)

LOAD P IN GM.	QUENCHING TEMPERATURE T_Q = 623°K							
	$A_k \times 10^{-4}$	$B_k \times 10^{2}$	$A_k B_k \times 10^{-2}$	$D_k \times 10^{-2}$	$\frac{P}{B_k} \times 10^{-2}$	$A_k P \times 10^{-2}$	$E_k \times 10^{2}$	$\frac{D_k E_k}{14230} \times 10^{-2}$
30	1.22	1.22	1.49	1.43	24.59	0.37	34.82	0.35
40	0.89	1.67	1.49	1.50	23.95	0.36	33.89	0.36
50	0.69	2.15	1.49	1.54	23.25	0.34	32.84	0.35
60	0.57	2.63	1.50	1.47	22.81	0.34	32.34	0.33
70	0.48	3.14	1.50	1.39	22.29	0.34	31.59	0.31
80	0.41	3.63	1.49	1.47	22.04	0.33	31.32	0.32
100	0.32	4.63	1.48	1.50	21.60	0.32	30.62	0.32
120	0.26	5.71	1.48	1.42	21.01	0.31	28.83	0.30
140	0.22	6.75	1.48	1.47	20.74	0.31	29.44	0.30
160	0.19	7.76	1.47	1.60	20.62	0.30	29.27	0.33
Mean	-	-	1.49	1.47	22.29	0.33	31.59	0.33

TABLE 8.10.4 (KNOOP INDENTER)

LOAD P IN GM.	QUENCHING TEMPERATURE $T_Q = 673^{o}K$							
	$A_k \times 10^{-4}$	$B_k \times 10^{2}$	$A_k B_k \times 10^{-2}$	$D_k \times 10^{-2}$	$\frac{P}{B_k} \times 10^{-2}$	$A_k P \times 10^{-2}$	$E_k \times 10^{2}$	$\frac{D_k E_k}{14230} \times 10^{-2}$
30	1.26	1.22	1.54	1.55	24.59	0.38	34.92	0.38
40	0.90	1.72	1.54	1.32	23.26	0.36	33.20	0.31
50	0.71	2.17	1.54	1.48	23.04	0.36	32.81	0.34
60	0.58	2.65	1.54	1.50	22.64	0.35	32.20	0.34
70	0.49	3.14	1.54	1.53	22.29	0.34	31.75	0.34
80	0.42	3.62	1.53	1.60	22.10	0.34	31.42	0.35
100	0.33	4.67	1.54	1.53	21.41	0.33	30.49	0.33
120	0.27	5.74	1.55	1.50	20.90	0.32	29.81	0.31
140	0.23	6.74	1.55	1.64	20.77	0.32	29.61	0.34
160	0.20	7.82	1.56	1.63	20.46	0.32	29.16	0.33
Mean	-	-	1.54	1.52	22.15	0.34	31.53	0.34

TABLE 8.10.5 (KNOOP INDENTER)

LOAD P IN GM.	QUENCHING TEMPERATURE T_Q = $773^{\circ}K$							
	$A_k \times 10^{-4}$	$B_k \times 10^{-4}$	$A_k B_k \times 10^{-2}$	$D_k \times 10^{-2}$	$\frac{P}{B_k} \times 10^{-2}$	$A_k P \times 10^{-2}$	$E_k \times 10^{2}$	$\frac{D_k E_k}{14230} \times 10^{-2}$
30	1.16	1.28	1.48	1.15	23.44	0.35	33.34	0.27
40	0.87	1.72	1.49	1.45	23.25	0.35	33.14	0.34
50	0.67	2.22	1.48	1.36	22.52	0.33	32.10	0.31
60	0.55	2.70	1.48	1.43	22.22	0.33	31.65	0.32
70	0.47	3.16	1.48	1.60	22.15	0.33	31.50	0.35
80	0.40	3.71	1.48	1.45	21.56	0.32	30.69	0.31
100	0.31	4.74	1.47	1.49	21.09	0.31	30.02	0.31
120	0.26	5.74	1.49	1.62	20.90	0.31	29.71	0.34
140	0.22	6.86	1.51	1.53	20.41	0.31	29.01	0.31
160	0.19	7.90	1.50	1.64	20.25	0.30	28.81	0.33
Mean	-	-	1.48	1.47	21.78	0.32	30.99	0.32

TABLE 8.10.6 (VICKERS INDENTER)

LOAD P IN Gm.	QUENCHING TEMPERATURE $T_Q = 303^{o}K$							
	$A_v \times 10^{-4}$	$B_v \times 10^{2}$	$A_vB_v \times 10^{-2}$	$D_v \times 10^{-2}$	$\frac{P}{B_v} \times 10^{-2}$	$A_vP \times 10^{-2}$	$E_v \times 10^{2}$	$\frac{D_vE_v}{1854.4} \times 10^{-2}$
30	9.54	0.88	8.40	8.30	34.09	2.86	6.30	2.82
40	6.87	1.23	8.40	7.40	32.52	2.75	6.05	2.41
50	5.39	1.56	8.40	7.50	32.05	2.69	5.93	2.40
60	4.36	1.93	8.40	6.80	31.09	2.62	5.76	2.11
70	3.72	2.26	8.40	7.80	30.97	2.60	5.73	2.41
80	3.19	2.63	8.40	7.10	30.42	2.55	5.63	2.15
100	2.50	3.36	8.40	7.10	29.76	2.50	5.51	2.11
120	2.06	4.09	8.40	7.40	29.34	2.47	5.43	2.17
140	1.73	4.85	8.40	7.30	28.86	2.42	5.34	2.10
160	1.49	5.66	8.40	6.80	28.27	2.38	5.23	1.92
Mean	-	-	8.40	7.30	30.74	2.58	5.69	2.26

TABLE 8.10.7 (VICKERS INDENTER)

LOAD P IN Gm.	QUENCHING TEMPERATURE $T_Q = 573^{\circ}K$							
	$A_v \times 10^{-4}$	$B_v \times 10^{2}$	$A_vB_v \times 10^{-2}$	$D_v \times 10^{-2}$	$\frac{P}{B_v} \times 10^{-2}$	$A_vP \times 10^{-2}$	$E_v \times 10^{2}$	$\frac{D_vE_v}{1854.4} \times 10^{-2}$
30	8.29	0.99	8.30	8.50	30.30	2.49	5.57	2.56
40	5.92	1.40	8.30	7.20	28.57	2.37	5.30	2.06
50	4.68	1.77	8.30	8.20	28.25	2.34	5.24	2.32
60	3.81	2.17	8.30	8.00	27.65	2.29	5.13	2.21
70	3.23	2.56	8.30	8.40	27.34	2.26	5.06	2.29
80	2.77	2.98	8.30	8.20	26.84	2.22	4.98	2.20
100	2.16	3.82	8.30	8.00	26.18	2.16	4.85	2.09
120	1.76	4.71	8.30	7.70	25.48	2.11	4.73	1.96
140	1.49	5.53	8.30	8.40	25.32	2.09	4.69	2.13
160	1.29	6.43	8.30	8.20	24.88	2.06	4.61	2.04
Mean	-	-	8.30	8.1	27.08	2.24	5.07	2.19

TABLE 8.10.8 (VICKERS INDENTER)

LOAD P IN Gm.	QUENCHING TEMPERATURE T_Q = $623^{\circ}K$							
	$A_v \times 10^{-4}$	$B_v \times 10^{2}$	$A_v B_v \times 10^{-2}$	$D_v \times 10^{-2}$	$\frac{P}{B_v} \times 10^{-2}$	$A_v P \times 10^{-2}$	$E_v \times 10^{2}$	$\frac{D_v E_v}{1854.4} \times 10^{-2}$
30	8.42	1.01	8.50	8.10	29.70	2.53	5.50	2.40
40	6.16	1.38	8.50	8.60	28.98	2.46	5.37	2.49
50	4.78	1.77	8.50	8.20	28.25	2.39	5.21	2.30
60	3.90	2.17	8.50	8.20	27.65	2.34	5.10	2.26
70	3.29	2.58	8.50	8.30	27.13	2.30	5.02	2.25
80	2.85	2.98	8.50	8.50	26.84	2.28	4.96	2.27
100	2.21	3.84	8.50	8.20	26.04	2.21	4.82	2.13
120	-	-	-	-	-	-	-	-
140	1.53	5.55	8.50	8.50	25.22	2.14	4.66	2.14
160	1.31	6.46	8.50	8.30	24.77	2.10	4.58	2.05
Mean	-	-	8.50	8.30	27.17	2.31	5.02	2.25

TABLE 8.10.9 (VICKERS INDENTER)

LOAD P IN Gm.	QUENCHING TEMPERATURE T_Q = 673 ^{o}K							
	$A_v \times 10^{-4}$	$B_v \times 10^{2}$	$A_v B_v \times 10^{-2}$	$D_v \times 10^{-2}$	$\frac{P}{B_v} \times 10^{-2}$	$A_v P \times 100^{-2}$	$E_v \times 10^{2}$	$\frac{D_v E_v}{1854.4} \times 10^{-2}$
30	8.03	1.09	8.70	8.40	27.52	2.41	5.11	2.32
40	5.63	1.55	8.70	6.40	25.81	2.25	4.78	1.65
50	4.55	1.92	8.70	8.80	26.04	2.27	4.83	2.29
60	3.71	2.36	8.70	8.80	25.42	2.23	4.72	2.24
70	3.12	2.80	8.70	8.90	25.00	2.18	4.64	2.22
80	2.70	3.24	8.70	9.20	24.69	2.16	4.58	2.27
100	2.09	4.18	8.70	8.90	23.92	2.09	4.44	2.13
120	1.68	5.21	8.70	8.00	23.03	2.02	4.28	1.85
140	-	-	-	-	-	-	-	-
160	1.24	7.05	8.70	9.30	22.69	1.98	4.21	2.11
Mean	-	-	8.70	8.50	24.90	2.18	4.62	2.12

TABLE 8.10.10 (VICKERS INDENDER)

LOAD P IN Gm.	QUENCHING TEMPERATURE $T_Q = 773^{\circ}K$							
	$A_v \times 10^{-4}$	$B_v \times 10^{2}$	$A_vB_v \times 10^{-2}$	$D_v \times 10^{-2}$	$\frac{P}{B_v} \times 10^{-2}$	$A_vP \times 10^{-2}$	$E_v \times 10^{2}$	$\frac{D_vE_v}{1854.4} \times 10^{-2}$
30	8.43	1.03	8.70	8.00	29.12	2.53	5.39	2.33
40	6.17	1.40	8.70	8.60	28.57	2.47	5.27	2.44
50	4.79	1.81	8.70	8.20	27.62	2.39	5.10	2.26
60	3.91	2.22	8.70	8.20	27.03	2.35	5.00	2.21
70	3.30	2.63	8.70	7.90	26.62	2.31	4.93	2.10
80	2.85	3.04	8.70	8.50	26.31	2.28	4.87	2.23
100	2.22	3.92	8.70	8.20	25.51	2.22	4.73	2.09
120	-	-	-	-	-	-	-	-
140	1.53	5.68	8.70	8.40	24.64	2.14	4.57	2.07
160	1.32	6.60	8.70	8.30	24.24	2.11	4.49	2.01
Mean	-	-	8.70	8.20	26.63	2.31	4.93	2.19

$$AB = \frac{PT_Q^{k + 0.09}}{d^2} \qquad \ldots\ldots\ldots (8.46)$$

$$A_k B_k = \frac{P_{TQ}^{k + 0.09}}{d_k^2} \qquad \ldots\ldots\ldots (8.46a)$$

$$A_v B_v = \frac{PT_Q^{k + 0.09}}{d_v^{\,2}} \qquad \ldots\ldots\ldots (8.46a)$$

$$AP = T_Q^{1 - m_1} \; a_2 \; d^{n_2 - 2} \qquad \ldots\ldots\ldots (8.47)$$

$$A_k P = T_Q^{1 - m_1} \; a_{2k} \; d_k^{n_2 - 2} \qquad \ldots\ldots\ldots (8.47a)$$

$$A_v P = T_Q^{1 - m_1} \; a_{2v} \; d_v^{n_2 - 2} \qquad \ldots\ldots\ldots (8.47b)$$

$$D = \frac{P}{d^2} \; d^{2 - n_2} \; T_Q^{1 - m_4} \qquad \ldots\ldots\ldots (8.48)$$

$$D_k = \frac{P}{d_k^{\,2}} \; d_k^{2 - n_2} \; T_Q^{1 - m_4} \qquad \ldots\ldots\ldots (8.48a)$$

$$D_v = \frac{P}{d_v^{\,2}} \; d_v^{2 - n_2} \; T_Q^{1 - m_4} \qquad \ldots\ldots\ldots (8.48b)$$

$$E = R\, T_Q^{1 - m_3}\, d^{n_2 - 2} \qquad \ldots\ldots\ (8.49)$$

$$E_k = 14230\, T_Q^{1 - m_3}\, d_k^{n_2 - 2} \qquad \ldots\ldots\ (8.49a)$$

$$E_v = 1854.4\, T_Q^{1 - m_3}\, d_v^{n_2 - 2} \qquad \ldots\ldots\ (8.49b)$$

$$DE = \frac{RP}{d^2}\, T_Q^{2 - m_3 - m_4} \qquad \ldots\ldots\ (8.50)$$

$$D_k E_k = \frac{14230\ P}{d_k^{\ 2}}\, T_Q^{2 - m_3 - m_4} \qquad \ldots\ldots\ (8.50a)$$

$$D_v E_v = \frac{1854.4\ P}{d_v^{\ 2}}\, T_Q^{2 - m_3 - m_4} \qquad \ldots\ldots\ (8.50b)$$

The means values of constants are summarized in Tables 8.11 and 8.12.

A careful study of mean values of 'constants' and their deviations from the corresponding individual observation clearly indicates that the deviations are within experimental errors. A glance at Tables 8.11 and 8.12 shows that,

$$D = AB \qquad \ldots\ldots\ldots\ (8.51)$$

TABLE - 8.11 (KNOOP INDENTER)

QUENCHING TEMPERATURE T_Q °K	$A_k B_k \times 10^{-2}$	$D_k \times 10^{-2}$	$A_k P \times 10^{-2}$	$\frac{D_k E_k}{14230} \times 10^{-2}$	$\frac{P}{B_k} \times 10^{-2}$	$E_k \times 10^2$	C_k	$\frac{C_k}{D_k} \times 10^2$
303	1.48	1.45	0.35	0.34	23.60	33.52	45.89	28.20
573	1.47	1.33	0.32	0.29	22.03	31.50	43.39	32.60
623	1.49	1.47	0.33	0.33	22.29	31.59	45.49	30.94
673	1.54	1.52	0.34	0.34	22.15	31.53	47.99	31.57
773	1.48	1.47	0.32	0.32	21.78	30.99	46.18	31.41
Mean	1.492	1.448	0.332	0.324	22.370	31.826	45.788	30.944
Coefficient of variation %	1.67	4.67	3.51	5.72	2.85	2.74	3.22	4.77
Values from graphs	1.41	1.49	0.32	0.315	22.76	30.07	45.90	30.805

TABLE 8.12 (VICKERS INDENTER)

QUENCHING TEMPERATURE $T^{o}K$	$A_vB_v \times 10^{-2}$	$D_v \times 10^{-2}$	$A_vP \times 10^{-2}$	$\frac{D_vE_v}{1854.4} \times 10^{-2}$	$\frac{P}{B_v} \times 10^{-2}$	$E_v \times 10^2$	C_v	$\frac{C_k}{D_k} \times 10^2$
303	8.4	7.3	2.58	2.26	30.74	5.69	40.12	5.49
573	8.3	8.1	2.24	2.19	27.08	5.07	39.97	4.93
623	8.5	8.3	2.31	2.25	27.17	5.02	40.87	4.92
673	8.7	8.5	2.18	2.12	24.90	4.62	41.07	4.83
773	8.7	8.2	2.31	2.19	26.63	4.93	39.92	4.87
Mean	8.520	8.080	2.324	2.202	27.304	5.066	40.390	5.008
Coefficient of variation percentage	1.88	5.18	5.89	2.28	6.99	6.88	1.19	4.86
Values from graphs	8.569	8.400	2.241	2.157	26.149	4.76	40.12	4.776

$$AP = \frac{DE}{R} \quad \ldots\ldots\ (8.52)$$

$$E = \frac{C}{D} \quad \ldots\ldots\ (8.53)$$

from tables 8.3 and 8.4

$$\frac{C_k}{C_v} = \frac{H_k}{H_v} \quad \text{for all temperatures}$$

Thus for all loads in HLR and for Knoop and Vickers indenters, the variation of hardness number H and the variation of hardness constant a_2 with quenching temperature and also with each other follow the equations,

$$HT_Q^{\ k} = C = \text{Constant} \quad \ldots\ldots\ (8.55)$$

$$a_2T_Q^{\ r} = D = \text{Constant} \quad \ldots\ldots\ (8.56)$$

$$a_2H^s = F = \text{Constant} \quad \ldots\ldots\ (8.57)$$

where k, r and s are numbers numerically less than unity. The signs for these constants decide the nature of ~~f~~ the crystal. For calcite they are negative as shown above. The constants in above equations have different values. Further quenching can also be carried out by bringing a crystal from very low temperature to room temperature. Thus for $T_Q = 1^oK$,

$$H = \text{constant} \quad \ldots\ldots\ (8.58)$$

$$a_2 = \text{constant} \quad \ldots\ldots\ (8.59)$$

These values can be considered to characterize a crystalline material. Thus for calcite, the quench hardness number and quench hardness constant are given by

$$H_k = 46.57 \text{ Kg - mm}^{-2} \qquad \ldots\ldots \quad (8.60)$$

and $$H_v = 41.44 \text{ Kg - mm}^{-2} \qquad \ldots\ldots \quad (8.61)$$

$$a_k = 1.47 \times 10^{-2} \text{ Kg - mm}^{-2} \qquad \ldots\ldots \quad (8.62)$$

and $$a_v = 1.84 \times 10^{-2} \text{ Kg - mm}^{-2} \qquad \ldots\ldots \quad (8.63)$$

8.3.2 Relation between hardness and electrical conductivity :

There are several temperature dependent crystal properties. One such property is electrical conductivity which varies in an exponential fashion with temperature. The comparision of electrical conductivity measured at temperature T to the microhardness value determined for the same quenching temperature could provide a clue about the possible relation between two quantities, hardness and electrical conductivity.

The values of electrical conductivity, σ_c, are given in table 8.13 (values are taken from Ph.D. thesis of R.T. Shah, 1976, M.S. University). Fig. 8.15 represents a graph of log $\sigma_c T$ versus $1/T$. The plot consists of three straight lines with different slopes and intercepts on the axes of log $\sigma_c T$ and $1/T$.

TABLE - 8.13*

T	σ_c	Log σ_cT	10^3/T.
453	4.395×10^{-12}	$\bar{9}.2991$	2.208
463	4.923×10^{-12}	$\bar{9}.3579$	2.160
473	5.603×10^{-12}	$\bar{9}.4227$	2.114
483	5.404×10^{-11}	$\bar{9}.7327$	2.070
493	1.213×10^{-11}	$\bar{8}.0840$	2.028
503	1.547×10^{-11}	$\bar{8}.1897$	1.988
513	1.804×10^{-11}	$\bar{8}.2562$	1.949
523	2.151×10^{-11}	$\bar{8}.3326$	1.912
533	4.686×10^{-11}	$\bar{8}.6798$	1.876
543	6.668×10^{-11}	$\bar{8}.8240$	1.842
553	1.014×10^{-10}	$\bar{7}.0200$	1.803
563	1.386×10^{-10}	$\bar{7}.1417$	1.776
573	1.660×10^{-10}	$\bar{7}.2200$	1.745
583	3.787×10^{-10}	$\bar{7}.3440$	1.715
593	6.715×10^{-10}	$\bar{7}.6000$	1.886
603	9.326×10^{-10}	$\bar{7}.7500$	1.658
613	2.051×10^{-9}	$\bar{6}.0995$	1.631
633	3.152×10^{-9}	$\bar{6}.3000$	1.580
648	4.879×10^{-9}	$\bar{6}.5000$	1.540

......contd.

* Taken from Ph.D thesis of R.T. Shah (1976)

TABLE - 8.13* (.... contd.)

T	σ_c	Log σT	10^3/T.
663	1.408×10^{-8}	$\bar{6}.9701$	1.508
678	1.484×10^{-8}	$\bar{5}.0025$	1.475
693	3.234×10^{-8}	$\bar{5}.3505$	1.443
708	5.441×10^{-8}	$\bar{5}.5856$	1.412
723	5.984×10^{-8}	$\bar{5}.6361$	1.383
738	1.087×10^{-7}	$\bar{5}.9047$	1.355
753	1.368×10^{-7}	$\bar{4}.0128$	1.328
768	1.995×10^{-7}	$\bar{4}.1852$	1.302
783	2.601×10^{-7}	$\bar{4}.3090$	1.277
798	3.324×10^{-7}	$\bar{4}.4237$	1.253
813	4.986×10^{-7}	$\bar{4}.6079$	1.230
828	5.567×10^{-7}	$\bar{4}.6636$	1.208
843	6.469×10^{-7}	$\bar{4}.7366$	1.186
858	7.252×10^{-7}	$\bar{4}.7940$	1.166
873	8.399×10^{-7}	$\bar{4}.8652$	1.145
888	9.768×10^{-7}	$\bar{4}.9382$	1.126
903	1.041×10^{-6}	$\bar{4}.9730$	1.107
918	1.140×10^{-6}	$\bar{3}.0196$	1.089
933	1.260×10^{-6}	$\bar{3}.0702$	1.072

* Taken from Ph.D. thesis of R.T. Shah (1976)

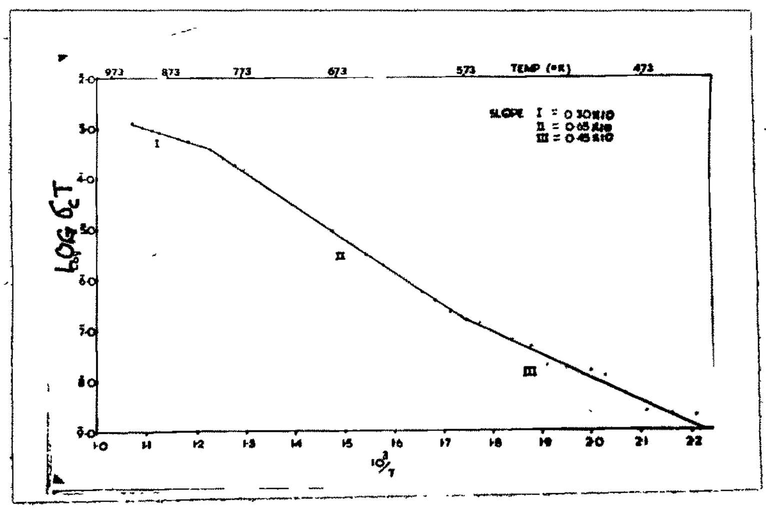

Fig. 8.15 Plot log ($\sigma_c T$) versus 1/T

It is clear from the general study of electrical conductivity of ionic crystals that the activation energies calculated for I, II and III parts of the graph are 0.90 ev for room temperature to 300°C, 1.3 ev for the region 310°C to 540°C and 0.6 ev for temperatures beyond 540°C. It is well known that calcite ($CaCO_3$) starts decomposing at a temperature of 500°C. The rate of decomposition increases with temperature. The thermal etching of calcite cleavage faces (Mehta, 1972) has shown very clearly that it could be effected and studied under controlled conditions only within a restricted range of temperature viz. 520°C to 560°C. Hence the third part of the graph indicating temperatures above 500°C shows the effect and onset of thermal etching. As a result of etching the slope of this line is comparatively less than those of lines belonging to II and III. In accordance with the general understanding of ionic crystals the jump energy is 0.90 ev while the formation energy for schottky defect is 0.8 ev.

It is known that the point defects which exists in crystal in thermal equilibrium, in contrast to thermodyna-mically unstable defects like dislocations and grain boundries, may contribute to mechanical properties through diffusion, e.g. creep at high temperatures. Hence it is desirable to review briefly the part played by point defects in 'hardening' crystalline materials. It is found that more direct effects of point defects on mechanical properties ~~of point defects~~, e.g. an increase in the yield stress, are caused by non-equilibrium concentrations of point defects, and on formation of their aggregates. In the present case non-equilibrium concentrations of point defects in calcite are produced by rapid cooling from high temperatures,the resulting hardening is called 'quench hardening' as distinct from radiation hardening produced by irradiation. The 'quench hardening is simpler amongst the two. The quenching experiments introduce the following few or all effects in a crystal :-

(i) Excess vacancies (equilibrium concentration of vacancies at higher temperature),

(ii) Possible aggregation of some vacancies.

(iii) Annihilation of vacancies.

(iv) Quenching strains.

(v) Pinning of vacancies at dislocations, grain boundries and impurities.

(vi) Effect of interstitials and their small aggregates.

The concentration and formation of energy of excess vacancies can be studied at low temperatures by measuring electrical resistivity. The main disadvantage in this procedure is possible aggregation or annihilation of some of the vacancies during quenching. Implicit in this method is the correction or avoidance of loss of vacancies together with any production of them e.g. by quenching strains and the effect of impurity and the formation of the more mobile vacancies. The quenching strains are associated with the production of vacancies. This will be clear from the following consideration.

During the quenching of the specimen, the surface is cooler than the inside and hence it is in tension while the inside is in compression. If the stress due to thermal gradient is large enough, the specimen will be deformed plastically. Since the yield stress is usually lower at higher temperature, the inside section of material will then undergo plastic deformation. When the quenching is completed and the temperature is again uniform, the plastically deformed inside material compresses the surface layers and vice versa. The thermal stresses thus set up are both axial and radial. Hence the deformation of the specimen is thus complex. Usually point defects are produced by deformation. Hence the production of vacancies by quenching strain must be taken into account in any assessment of the number of vacancies quenched into a crystal. Further the mechanical properties of a crystal are largely determined by the number, geometrical configurations, interactions and mobility of dislocations contained in it. The mobility of dislocations is mainly determined by their interactions with other defects, Structural and/or otherwise. It is this interaction which produces 'hardening'. This production will now be reviewed briefly.

Non-conservative motion of jogs on dislocation and annihilation of two parallel edge dislocations of opposite sign, one atomic plane apart, are the main mechanism suggested for point defect formation during deformation by mechanical means or by quenching. The non-conservative motion of jogs is possible both on edge dislocations and screw dislocations. For deformation, however, jogs on screw dislocations are more important. Jogs on screw dislocation are geometrically short segments of edge dislocations. The slip plane of these jogs is not the slip plane of the parent screw dislocation. Hence as the screw dislocation moves, jogs should move in a non-conservative manner along the screw. These fundamental mechanisms of point defect formation are well established geometrically, but the theory cannot predict as yet how many of particular species of defect are produced under certain conditions. This is a very difficult problem because the number and behaviour of moving dislocations are very complicated functions of the deformation temperature, the strain rate as well as other conditions of the specimen. A complete understanding of work hardening is required to solve this problem. Thus quenching produces dislocations, grain boundries segragation of impurities as well as point defects. It is also observed that a physical property suitable to detect the excess vacancies is also affected by plane and volume defects. Hence it is necessary to separate the effect of particular kind of defect from the effect of others. The procedure for effecting this discrimination varies in a finer way from specimen to specimen, materials to materials. This is not yet perfected for all types of materials. The interstitials act in somewhat similar fashion as mentioned for vacancies.

The above presents briefly the possible effects of quenching processes on the materials. It is now interesting to consider the effect of these processes on crystals. It is observed that no noticeable increase or change in hardness is found for quenched and aged metallic crystals. This is in marked contrast with the pronounced change in yield stress. The reason for this apparent contradiction is found in the observed stress-strain curve of the quenched hardened crystal i.e. the effect of quenching on hardening disappears after a moderate amount of deformation. Since hardness is a measure of resistance to deformation, microhardness measurements using very small loads might detect quench hardening. However use of small loads would determine the hardness of only the surface layers probably few microns deep. It may be remarked that even in the low load region, local deformation will be severe. Since the vacancies escape to the surface during quenching, no hardening is to be expected in the thin surface layers. It is therefore imperative to remove the surface layers in order to detect hardening using small load microhardness measurements. It is from this view that Aust et al, (1966) quenched zone-refined lead from near 300°C into water. Hardness was measured using a load of 1 gm, this resulted in a depth of indentation of about 3 μ . The specimen showed no hardening when tested without removing surface layers. Further hardening was observed when surface layers of 50 μ thickness were removed. They also found that the region near the grain boundry showed no hardening. This is most likely to be due to the escape of vacancies to grain boundries during quenching. Since the vacancies anneal out of the surface during quenching, the first few layers will not exhibit quenching effect. As calcite has a perfect cleavage, the quenched samples were cleaved and the hardness studies were carried out on these freshly cleaved specimens.

The graphs of log $T_{Q}d$ versus $1/T_{Q}$ and log $\sigma_{c}T$ versus $1/T$ for calcite crystals have close resemblence with one another (Fig. 8.16, 8.17, Tables 8.14, 8.15). Hence it appears that similar mechanisms are likely to operate in the crystal. Further, the plots of log $T_{Q}d$ versus $1/T_{Q}$ are parallel to one another except for the loads where maximum hardness is observed. Hence it can be conjectured that the point defects are mainly responsible for increased hardness of calcite crystals due to quenching. This is supported by the empirical relation between hardness and schottky defects in alkali halides at room temperature (Shukla and Bansigir, 1976). With the increase of applied load dislocations which are produced on cleavage face by indentation would start interacting with quenched-in point defects. As a result the effect of load on indenter is reflected in the lost parallelism of graphs near the loads where kink in log P vs log d graphs is observed. For higher loads, the graphs of log $T_{Q}d$ vs $1/T_{Q}$ are again parallel to one other. It is thus clear why the graph of hardness against load is divided into three regions. In the first region (oA of plot) the quenched-in point defects operate through grown and aged dislocations ignoring to a greater extent the contribution of fresh dislocations introduced by indentations ; at higher loads (BC portion of the graph) the freshly introduced dislocations are more active than grown and aged dislocations in 'hardening' the crystals. For intermediate loads (associated with portion

TABLE - 8.14 (KNOOP INDENTER)

P in gm.	Log $T_0 d_k$				
	303 K	573 K	623 K	673 K	773 K
2.5	3.8605	4.1595	4.1736	4.3377	4.3375
3.75	3.9313	4.2153	4.2368	4.2396	4.3516
5.00	3.9911	4.2326	4.2928	4.3377	4.3505
7.50	3.9967	4.2898	4.3153	4.3543	4.3902
8.75	4.0213	4.2992	4.3269	4.3709	4.3892
10.00	4.0824	4.3356	4.3622	4.3755	4.4035
12.50	4.0824	4.3545	4.3719	4.3908	4.4656
15.0	4.1027	4.3636	4.4000	4.4289	4.5114
20	4.1765	4.4581	4.4744	4.5279	4.6320
30	4.2630	4.5909	4.5938	4.6066	4.7393
40	4.3551	4.6532	4.6518	4.7161	4.7519
50	4.4269	4.7336	4.7209	4.7412	4.8210
60	4.4568	4.7431	4.7541	4.7186	4.8518
70	4.4956	4.7705	4.8051	4.8129	4.8616
80	4.5312	4.8079	4.8243	4.8350	4.9179
100	4.5832	4.8527	4.8725	4.8999	4.9663
120	4.6205	4.8933	4.9296	4.9495	4.9885
140	4.6573	4.9254	4.9580	4.9644	5.0403
160	4.6821	4.9834	4.9703	4.9980	5.0555

TABLE - 8.15 (VICKERS INDENTER)

P in gm.	Log $T_Q d_V$				
	303°K	573°K	623°K	673°K	773°K
2.50	3.4664	3.7181	3.7244	3.7300	3.8181
3.75	3.4541	3.7693	3.7945	3.8002	3.8882
5.00	3.5360	3.7995	3.8198	3.8492	3.9093
7.50	3.5818	3.8670	3.9034	3.9426	3.9957
8.75	3.6124	3.9092	3.9289	3.9485	4.0090
10.00	3.6487	3.9165	3.9409	3.9698	4.0343
12.50	3.6729	3.9622	3.9766	3.9979	4.0645
15.00	3.7175	4.0063	4.0112	4.0280	4.1030
20.00	3.7323	4.0395	4.0732	4.0979	4.1648
30.00	–	4.1273	4.1748	4.2147	4.2685
40.00	3.9435	4.2053	4.2274	4.2642	4.3195
50.00	3.9912	4.2605	4.2943	4.3266	4.3878
60.00	4.0589	4.3083	4.3398	4.3703	4.4322
70.00	4.0732	4.3356	4.3721	4.4056	4.4655
80.00	4.1175	4.3739	4.3982	4.4290	4.4913
100.0	4.1691	4.4315	4.4620	4.4927	4.5553
120.0	4.2050	4.4857	–	4.5652	–
140.0	4.2445	4.5012	4.5348	–	4.6286
160.0	4.2922	4.5387	4.5734	4.5974	4.6664

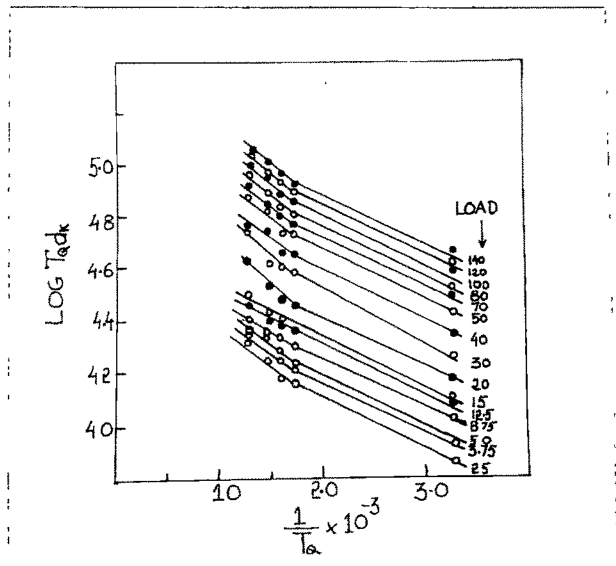

Fig. 8.16 Plot of log $T_Q d_k$ versus $1/T_Q$ for various loads.

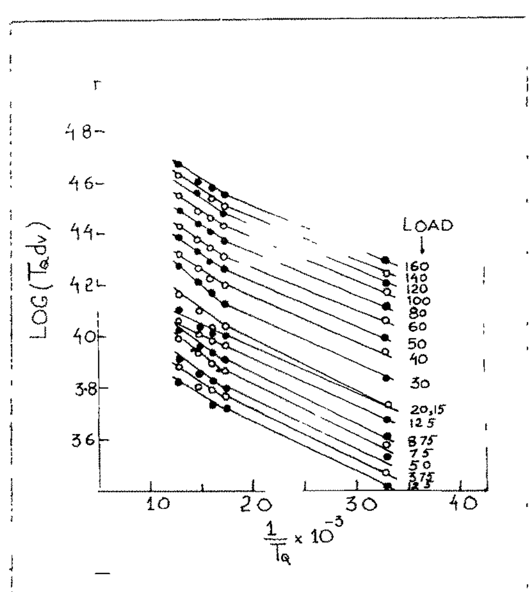

Fig. 8.17 Plot of log $T_Q d_v$ versus $1/T_Q$ for various loads.

AB of the graph) there appears to be a complicated interaction between quenched-in point defects, aged dislocations and freshly introduced dislocations, resulting in the non-linear behaviour of hardness versus load. It should be remarked here that the line of demarcation between low loads and intermediate loads, between intermediate loads and high loads is not well defined.

The value of load at which hardness acquires a maximum value is not constant but changes with the quenching temperature. It shifts towards the lower load value with higher quenching temperature. This is more clear from the graph of log P vs log d and can be inferred to a certain extent, from the graphs of hardness vs load.

It is clear from the above discussions that the behaviour of hardness is similar to that of conductivity for various quenching temperatures. Further the low load hardness values in the first region are governed by nature, distribution and concentration of quenched-in point defects, and their interactions with grown and aged dislocations. Further the thrid region BC of the plot of hardness vs load is governed mainly by freshly introduced dislocations. Hence it is desirable to discuss the comparative behaviour of these two quantities with respect to temperature. Out of several combinations of these quantities to form different functions, the function (log $\sigma_c/\bar{H}$)/log T has almost a constant value (Table 8.16) in high load region. Hence the graph of log $\sigma_c/\bar{H}$ versus log T are plotted for high load region (Fig. 8.18). The graph is a straight line for knoop as well as vickers hardness numbers. Thus, it is clear that for a given crystal $\sigma_c/\bar{H}$ has a constant value at a constant temperature for high load region. Since electrical conductivity is proportional to the diffusion constant. (Nernst-Einstein equation) it can be concluded that for a given ionic crystal, the ratio of diffusion constant to hardness (number) at a constant temperature is constant in high load region. This also indicates that defect structure of the material in general and in particular equilibrium concentration of point defects at the quenching temperature for the same material for which two quantities are determined is more or less identical.

To verify the results obtained from hardness studies, the data on hardness is combined with the data on electrical conductivity. The electrical conductivity of calcite is basically ionic in character. At temperature $T^{o}K$ it is given by

$$\sigma_c = \frac{\sigma_{oc}}{T} \exp(-E/kT) \qquad \ldots\ldots\ldots (8.64)$$

where σ_{oc} is a constant independant of temperature and K is Boltzmann's constant.

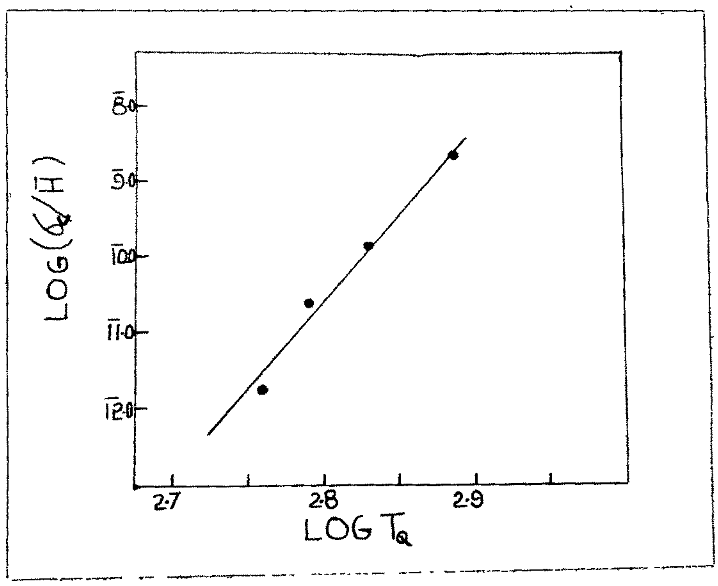

Fig. 8.18 Plot of log ($\sigma_c/\bar{H}$) vs log T_Q

TABLE 8.16

T_Ω	log T_Ω	$\bar{H}_k$	$\bar{H}_v$	σ_c	$\log \frac{\sigma_c}{\bar{H}_k}$	$\log \frac{\sigma_c}{\bar{H}_v}$
573	2.7582	92.99	85.68	1.66×10^{-10}	$\bar{12}.2517$	$\bar{12}.2873$
623	2.7944	98.44	88.46	2.5×10^{-9}	$\bar{11}.4048$	$\bar{11}.4512$
673	2.8280	104.84	89.71	1.45×10^{-8}	$\bar{10}.1409$	$\bar{10}.2086$
773	2.8882	102.58	88.69	2.3×10^{-7}	$\bar{9}.3507$	$\bar{9}.4139$

TABLE 8.17

$T_Q\,^oK$	σ_c	$\frac{\sigma_c T_Q^{\,1-k}}{H_k}$	$\frac{\sigma_c T_Q^{\,1-k}}{H_v}$	$\log \frac{\sigma_c T_Q^{\,1-k}}{H_k}$	$\log \frac{\sigma_c T_Q^{\,1-k}}{H_v}$	$\frac{1}{T} \times 10^{-3}$
573	1.66×10^{-10}	21.91×10^{-10}	23.78×10^{-10}	$\bar{9}.3406$	$\bar{9}.3762$	1.74
623	2.5×10^{-9}	34.24×10^{-9}	38.10×10^{-9}	$\bar{8}.5345$	$\bar{8}.5809$	1.60
673	1.45×10^{-8}	20.32×10^{-8}	23.75×10^{-8}	$\bar{7}.3079$	$\bar{7}.3756$	1.48
773	2.3×10^{-7}	38.48×10^{-7}	44.5×10^{-7}	$\bar{6}.5852$	$\bar{6}.6484$	1.29

Combination of eq. (8.64) with HT^k = constant yields,

$$\log \frac{\sigma_c T^{1-k}}{\bar{H}} = \frac{-E}{KT} \log_{10} e + \log D \quad ..... (8.65)$$

where log D is a constant given by $\log \sigma_{oc} - \overline{\log_{10} A}$. It is obvious that if the value of 'k' calculated from hardness studies is substituted in eq. (8.65), a plot of $\log \frac{\sigma_c T^{1-k}}{\bar{H}}$ vs. 1/T (Fig. 8.19, table 8.17) should be similar in all respects to that of conductivity plot except for the intercept. The value of activation energy calculated using eq. (8.65) is 1.3 ev. in accordance with the value of activation energy calculated using conductivity data alone in the temperature range of 300°C to 500°C.

8.4 CONCLUSIONS :

(i) The comparative study of hardness and electrical conductivity of the cleavaged specimens at different temperatures indicate that the plot between hardness and load can be qualitatively divided into three portions viz. low load region corresponding to linear part, intermediate load region corresponding to non-linear part and high load region corresponding to linear portion of the graph. It is also shown qualitatively that (a) in low load region the quenched-in point defects operate through their interactions

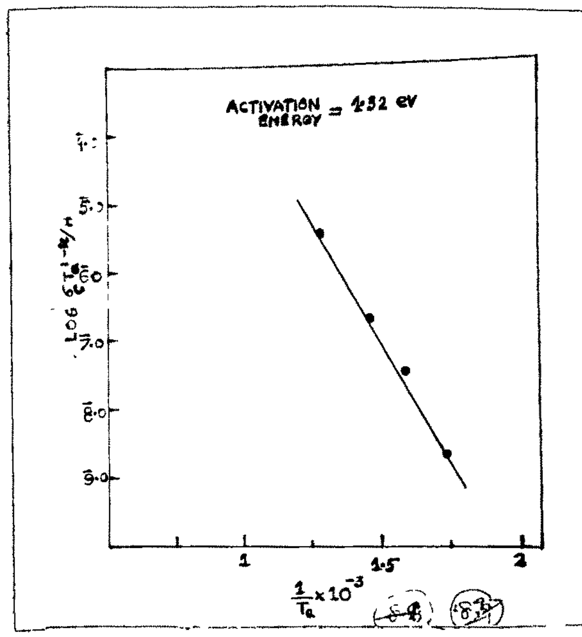

Fig. 8.19 Plot of log ($\sigma_c T^{1-k/\bar{H}}$) vs 1/T

with grown and aged dislocations, (b) the complicated interactions between quenched-in point defects, grown, aged and freshly introduced dislocations give rise to non-linear portion and (c) the freshly introduced dislocations by indentations at high loads control the linear portion of the graph.

(ii) Hardness depends upon quenching temperature. A relation between hardness and quenching temperature is given by

(a) $HT_Q^{\,k}$ = constant where $k = -0.12$ for calcite.

(b) $a_2 T_Q^{\,r}$ = constant where $r = -0.03$,, ,,

(c) $a_2 H^s$ = constant where $s = -0.25$ for calcite.

(iii) The ratio of electrical conductivity to hardness (number) of calcite crystal is constant at a constant temperature in high load region.

(iv) Knoop hardness number has higher values than Vickers hardness number at any given temperature.